ACID PRECURSOR INCORPORATED NANOCAPSULES AND SOLID POLYMER NANOPARTICLES FOR ENHANCED OIL RECOVERY

A Thesis
Presented to the Faculty of the Graduate School
of Cornell University
in Partial Fulfillment of the Requirements for the Degree of
Master of Science

by
Sidi Duan
August 2019

BIOGRAPHICAL SKETCH

M.S. 2017- Department of Materials Science and Engineering, Cornell University

B.S. 2013-2017 Department of Building Science, Tsinghua University

ACKNOWLEDGMENTS

First, I would like to show my deepest gratitude to my advisor Professor Emmanuel Giannelis, who guided me through my project and encouraged me whenever I'm in doubt. Second, I want to acknowledge my committee member Professor Christopher Ober for his help and support. I would also like to thank all the students and postdocs in the group for being such reliable colleagues at work and such warm-hearted friends in life. My sincere appreciation also goes to all the new friends I made here at Cornell, especially my roommate Qi, who made my life so much more colorful even in the snowiest weather. I must also express my profound gratitude to my parents and my grandma for their unconditioned love and support. Even though I'm far away from home, our hearts are close together. Last but not least, I want to thank Yichen for going through all the hard times and enjoying all the good times with me.

PREFACE

This Master thesis was written from January 2019 to August 2019 and was submitted to the Department of Materials Science and Engineering of Cornell University. This work provides a novel way of conducting Enhanced Oil Recovery.

I would like to express my appreciation to Professor Emmanuel Giannelis and Professor Christopher Ober for their advice and encouragement. I also want to thank Genggeng Qi, Katie Li, Wenyang Pan, Xiao Liu, and Apostolos Enotiadis for those helpful discussions.

07/27/2019

Sidi Duan

TABLE OF CONTENTS

LIST OF TABLES

LIST OF FIGURES

ABSTRACT

Secondary and tertiary enhanced oil recovery address the issue of reduced oil production over the years. To facilitate the recovery of residual oil in the reservoir, well stimulation using strong acids, e.g. concentrated HCl, is usually used to enlarge the pores trapping oils in the formation. However, the application of strong acids suffers from short penetration depth as a result of fast reaction with the rock (e.g. carbonate) formation. Herein we describe two new approaches, in which encapsulated and polymerized acid precursors are used to deliver both acids and surfactants in a controlled manner for more efficient enhanced oil recovery. In comparison with the common industry methods, our methods allow for controlled acid release so that deeper acid penetration can be achieved. Meanwhile, the acid can then act as surfactant after dissolving rock, which helps to free the residual oil in the reservoir.

1. Introduction

According to "Statistical Review of World Energy (2019)" [1], the largest part of world primary energy consumption is oil, which takes up more than 30% of the total 13864.9 million tons oil equivalent. [2] It is increasingly hard to meet the energy demand as the oil consumption goes up year after year, while the discovery of new oil field slows down. [3] One way of alleviating the problem is to extract the remaining 60% to 80% of the oil left in the reservoir after primary and secondary oil recovery.

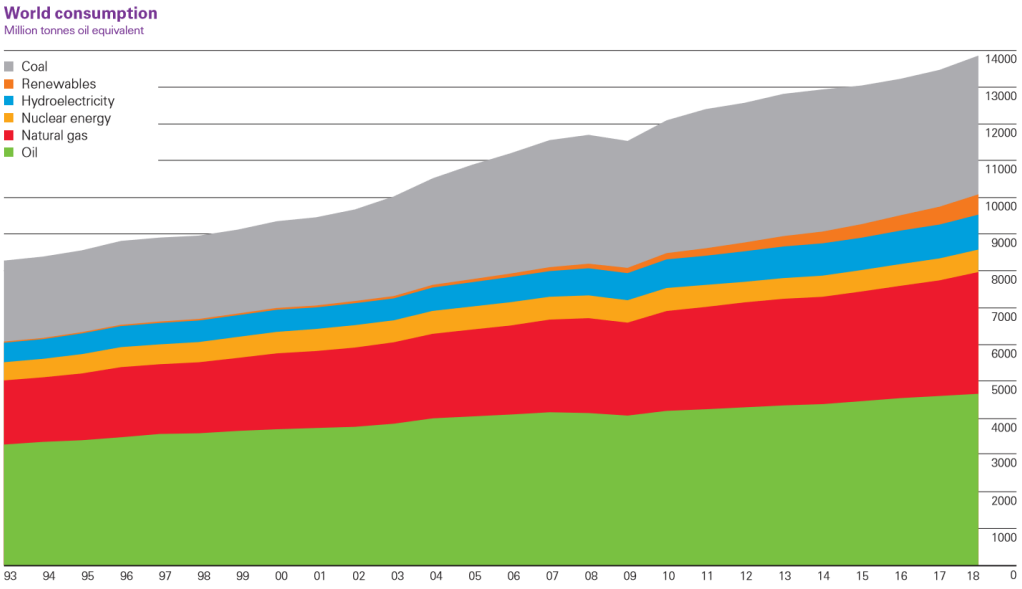

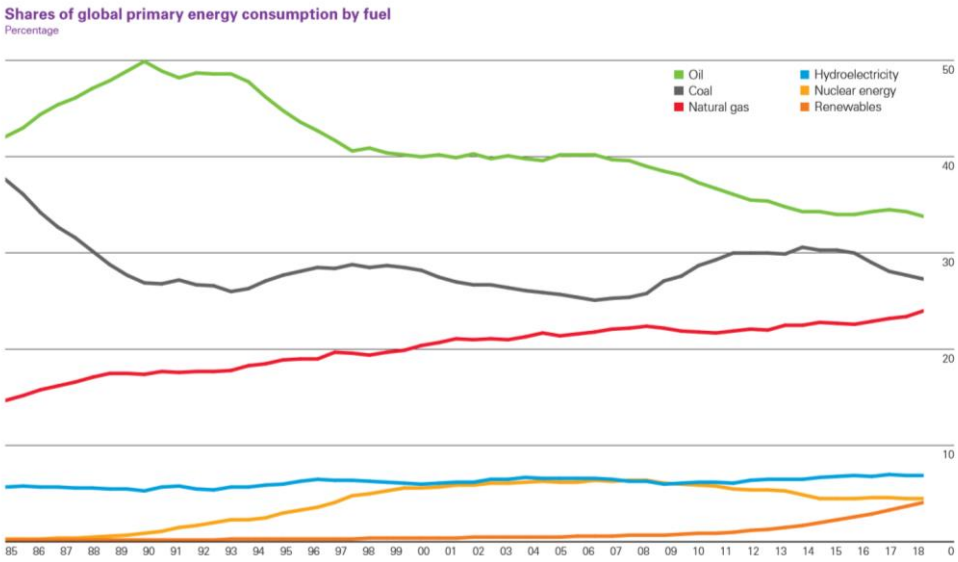

Figure 1 (Top) World's energy consumption from 1993 to 2018.[1] (bottom) shares of global primary energy consumption by fuel.[1]

Tertiary oil recovery, also known as enhanced oil recovery (EOR), promises to produce 30% to 60% of the total oil in the reservoir. EOR methods include well stimulation, chemical flooding, miscible flooding, thermal methods, immiscible gas injection methods, etc. [4] This study mainly focuses on acid stimulation methods, while also touch on the surfactant utilized in chemical flooding.

Acid stimulation techniques have been used for over a hundred years, and is still widely used today. [5] The most common acid injected is hydrochloric acid, for its affordable price and ability to dissolve carbonate rock. However, it suffers from fast reaction rate under high temperatures resulting in short penetration distances. Sometimes inhibitors are needed to prevent damaging oil field casings. [6] Several other methods have been developed addressing these problems. Harris et al. proposed a way of generating organic acid in-situ by using esters and enzymes,

which involves hazardous and high cost chemicals. [7] Fredd et al. used EDTA, one of the chelating agents in the EDTA family, to segregate metals in carbonate rock. Although the chelatants have slower corrosion rate, which results in less amount of inhibitors required, this method still suffers from high cost, and it might do harm to the environment by making heavy metals in the oil field more mobile. [8] Retarding the acid by emulsification slows down the reaction rate of hydrochloric acid, because it lowers the diffusion coefficient of the emulsified acid. However, experiments done by Tupã et al. (2016) show that the reaction time after emulsification is still short compared with the time it takes for oil to travel through the oil field. [9] In order for the less hazardous and more affordable hydrochloric acid to work, the reaction rate needs to be further slowed down. [10]

Surfactant flooding aims to mobilize oil trapped in porous rocks by lowering interfacial tension between water and oil. [11] Previous research shows that sulfonate surfactants tend to remain effective under high temperature for a longer time. The presence of sulfonate group also has the advantage of stabilizing the emulsion in high salinity environment, especially with high concentration divalent ions. [12] Hirasaki et al. suggested that the incorporation of alcohol as a cosurfactant prevents the microemulsion from phase-separation. [13] There is a wide choice of sulfonate surfactants and cosurfactants available in the literature, which are summarized in Table 1. The combination of acid precursor and surfactant provides a two-pronged approach to enhanced oil recovery.

Table 1 Commonly used surfactants and cosurfactants in surfactant flooding.

Surfactant	Cosurfactant	Reference
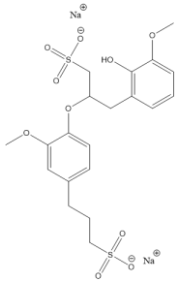 sodium ligno sulfonate	Alcohol from palm oil and sugar industries	[14]
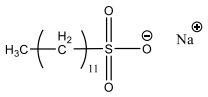 sodium dodecyl sulfonate	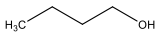 n-butanol	[15]
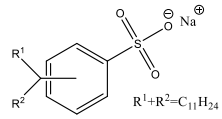 sodium dodecylbenzene sulfonate		
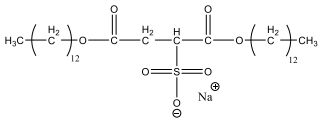 di-tridecyl sulfosuccinic acid ester	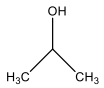 isopropyl alcohol	[16]
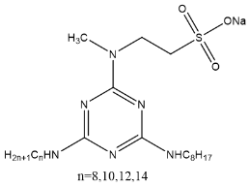 double long-chain 1,3,5-triazine		[17]
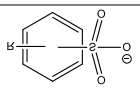 alkyl benzene sulfonate	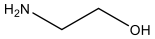 monoethanolamine	[18]

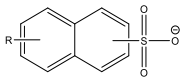

alkyl naphthalene sulfonate

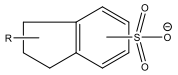

alkyl indane sulfonate

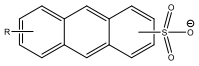

alkyl phenanthrene sulfonate

The harsh environment in the oil field poses huge challenges to EOR. High salinity and high temperature (80-120°C) render many types of surfactants ineffective and make it difficult for particles and polymers to stay stable in the reservoir. Certain porous carbonate rock, where the remaining oil is trapped has a pore diameter around 100 nm or less. This brings about a hard-to-meet limitation on particle size of possible materials to be used. Another characteristic of oil field is that the distance between injection well and production well can range from several hundred feet to miles, which requires the materials chosen to react slowly and remain effective for days or even months. [23]

In this thesis, we focus on two new ways of acid simulation via encapsulation or polymerization of acid precursors. The nanocapsules are made by interfacial polymerization, while the nanospheres are made by emulsion polymerization. The acid precursor, after injection into the oil reservoir, reacts with water and generates acid in-situ. As the capsules travel along in the oil field, they release acid at a

controlled rate, and the product of the acid reacted with rock can act as a surfactant.

The nanocapsules used in this work are around 200nm, and able to stay dispersed in saline water for a considerable amount of time until they are dissolved slowly to release the acid. The acid precursor is intact until the capsule shell dissolves or breaks, after which it releases acid upon reacting with water and promotes the emulsification of the oil/water mixture. To analyse the effect of the salinity of the environment, several tests were carried out in brine. Results suggest that controlled release of acid and emulsification effect can be achieved in saline water. The nanospheres synthesized in this work are down to around 100nm, and are able to stay dispersed in saline water under high temperature for a long time. Accelerated hydrolysis results proved the possibility of slow in-situ acid release and the capability of hydrolysed polymer to provide effective emulsion.

2. Acid Incorporated Nanocapsules for Enhanced Oil Recovery

2.1. Materials and Methodology

2.1.1. Interfacial Polymerization Mechanism

Interfacial polymerization is a type of step-growth polymerization, which produces thin films or capsules. In our case, an oil-in-water emulsion is first obtained, with two types of monomers dissolved in the oil and aqueous phase, respectively. When the monomers meet at the oil-water interface, polymerization occurs and a shell around the oil droplets gradually forms. [19] A schematic of the described process is shown in Figure 2.

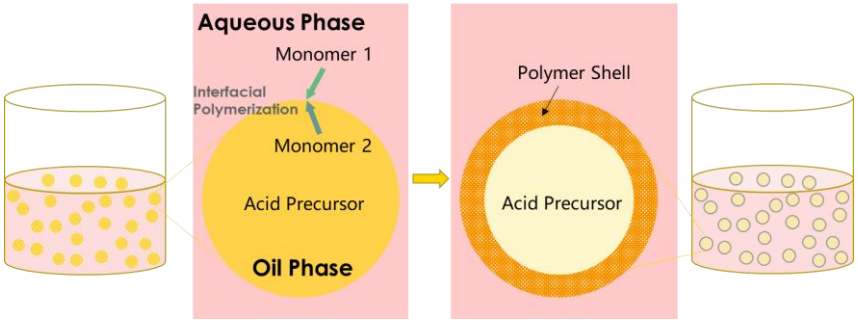

Figure 2 Schematic of interfacial polymerization

Similar systems were already reported in the literature. Bouchemal et al. synthesized poly(ether urethane) nanocapsules by interfacial polymerization with diisocyanate and polyethylene glycol oligomers. The size of the nanocapsules produced ranges from 232nm to 615nm. [20] Liang et al. used toluene-2,4-diisocyanate and ethylenediamine to produce microcapsules with diameter of 20-35μm. [21]

2.1.2. Materials Used

2.1.2.1. Surfactants

Sodium dodecyl sulfate (SDS), dodecyl dimethyl(3-sulfopropyl) ammonium hydroxide (DDSA), and cetyl trimethyl ammonium bromide (CTAB) were obtained from Sigma Aldrich. DOWFAX® 2a1 was supplied by Dow Chemical Company.

2.1.2.2. Costabilizer

Hexadecane was obtained from Sigma Aldrich.

2.1.2.3. Aqueous Phase Monomer

Lysine, diethylenetriamine (DETA), Aspartic Acid and 2,4-diaminobenzenesulfonic acid (DBSA) were obtained from Sigma Aldrich.

2.1.2.4. Oil Phase Solvent

Xylenes was obtained from Sigma Aldrich.

2.1.2.5. Oil Phase Monomer

Toluene diisocyanate (TDI) and isophorone diisocyanate (IDI) were obtained from Sigma Aldrich.

2.1.2.6. Acid Precursors

1-octanesulfonyl chloride, 1-dodecanesulfonyl chloride, 1-hexadecanesulfonyl chloride, 4-tert-butylbenzenesulfonyl chloride, and biphenyl-4-sulfonyl chloride

were obtained from Sigma Aldrich.

2.1.2.7. Saline Water

Sodium chloride, calcium chloride dihydrate, and magnesium chloride hexahydrate were obtained from Sigma Aldrich. Concentrated saline water stock was prepared by adding sodium chloride (74.59g), calcium chloride dihydrate (49.79g) and magnesium chloride hexahydrate (13.17g) into 750mL of deionized water. Unless stated otherwise the saline water used for the synthesis and testing experiments was made by mixing 3 parts of the above stock solution with one part deionized water.

2.1.2.8. Crude Oil

Crude oil was provided by Saudi Aramco.

2.1.2.9. Nanocapsules Preparation

The synthesis of neat nanocapsules without the acid precursor consists of 12g of deionized water or saline water, 0.1g of surfactant, 1.79mmol of aqueous phase monomer, 0.25g of hexadecane, 2.6g of xylenes, and 2.16mmol of oil phase monomer following these steps.

a. The ingredients for the aqueous phase, including surfactant, costabilizer, monomers, and deionized water/saline water were mixed and stirred at 50°C for 1 hour.
b. The ingredients for the oil phase, including the organic solvent and monomers, were mixed to form a homogeneous solution.

c. The oil phase was added into the aqueous phase solution while being ultrasonicated by Branson Digital Sonifier 450 and stirred for 3 minutes.

d. The mixed solution was stirred overnight at 200rpm at room temperature.

The synthesis of the nanocapsules with the acid precursor consists of 12g of deionized water or saline water, 0.1g of surfactant, 1.79mmol of aqueous phase monomer, 0.25g of hexadecane, 1.3g of xylenes, 4.84mmol of acid chloride, and 2.16mmol of oil phase monomer and following the above steps for the neat nanocapsules except that the acid precursor was mixed into the oil phase in step b.

2.1.3. Nanocapsules Size Measurement

Size distribution of the nanocapsules was measured by dynamic light scattering (DLS) using Malvern Zetasizer Nano ZS. Samples were diluted with deionized water unless otherwise stated. Particle size distribution, number average size, and PDI were obtained from these measurements.

2.1.4. Nanocapsules Morphologies

The morphologies of the nanocapsules was determined by scanning electron microscopy (SEM) using Tescan Mira3 FESEM. SEM samples were prepared by sticking conductive copper tape onto a metal stage and dropping a few droplets of the solution onto the copper tape. The samples were imaged after the solvent evaporated and the films dried.

2.1.5. Stability Tests

The stability of the samples was evaluated by letting the solution stand and observing the process of phase separation or precipitation. For tests in salinity water a solution containing a total of 110,000 ppm salts (NaCl, $CaCl_2$ and $MgCl_2$) was used. For tests at high temperature, samples in sealed glass vials were kept in an oven at 80-90°C for the appropriate time.

2.1.6. Hydrolysis Rate Measurement

The hydrolysis rate of either the acid precursors or the acid precursor incorporated into the nanocapsules was evaluated by measuring the pH changes during hydrolysis using a Hanna pH meter. For the acid precursor hydrolysis tests, 5mmol of acid precursor was added into 10g of deionized water, and the mixture was heated up to 80°C under stirring. For nanocapsule hydrolysis tests, 10g of sample solution with 5mmol of acid precursor encapsulated was heated up to 80°C under stirring.

2.1.7. Emulsifying Ability Tests

1g crude oil was added into the hydrolyzed solution, and the mixture was ultrasonicated using VWR Aquasonic 150D. Images were taken after different standing time to record the process of phase separation.

2.2. Results and Discussion

2.2.1. Influence of Salinity

The first step optimizing the synthesis protocol is to determine the key parameters for achieving the desired capsule morphology. Table 2 summarized the experiments

conducted in both deionized water and saline water.

Table 2 Synthesis protocol for nanocapsules.

NO.	Surfactant	Monomer1	Monomer2	Aqueous Phase Solvent	Oil Phase Solvent	Oil Phase Cosolvent
1	SDS	Lysine	IDI	DI	Xylene	Hexadecane
2	SDS	Lysine	TDI	DI	Xylene	Hexadecane
3	SDS	DBSA	IDI	DI	Xylene	Hexadecane
4	SDS	DBSA	TDI	DI	Xylene	Hexadecane
5	CTAB	Lysine	IDI	DI	Xylene	Hexadecane
6	CTAB	Lysine	TDI	DI	Xylene	Hexadecane
7	CTAB	DBSA	IDI	DI	Xylene	Hexadecane
8	CTAB	DBSA	TDI	DI	Xylene	Hexadecane
9	DDSA	Lysine	IDI	DI	Xylene	Hexadecane
10	DDSA	Lysine	TDI	DI	Xylene	Hexadecane
11	DDSA	DBSA	IDI	DI	Xylene	Hexadecane
12	DDSA	DBSA	TDI	DI	Xylene	Hexadecane
13	DOWFAX	Lysine	IDI	DI	Xylene	Hexadecane
14	DOWFAX	Lysine	TDI	DI	Xylene	Hexadecane
15	DOWFAX	DBSA	IDI	DI	Xylene	Hexadecane
16	DOWFAX	DBSA	TDI	DI	Xylene	Hexadecane
17	DDSA	Lysine	IDI	SW	Xylene	Hexadecane
18	DDSA	Lysine	TDI	SW	Xylene	Hexadecane
19	DDSA	DBSA	IDI	SW	Xylene	Hexadecane
20	DDSA	DBSA	TDI	SW	Xylene	Hexadecane
21	DOWFAX	Lysine	IDI	SW	Xylene	Hexadecane
22	DOWFAX	Lysine	TDI	SW	Xylene	Hexadecane
23	DOWFAX	DBSA	IDI	SW	Xylene	Hexadecane
24	DOWFAX	DBSA	TDI	SW	Xylene	Hexadecane

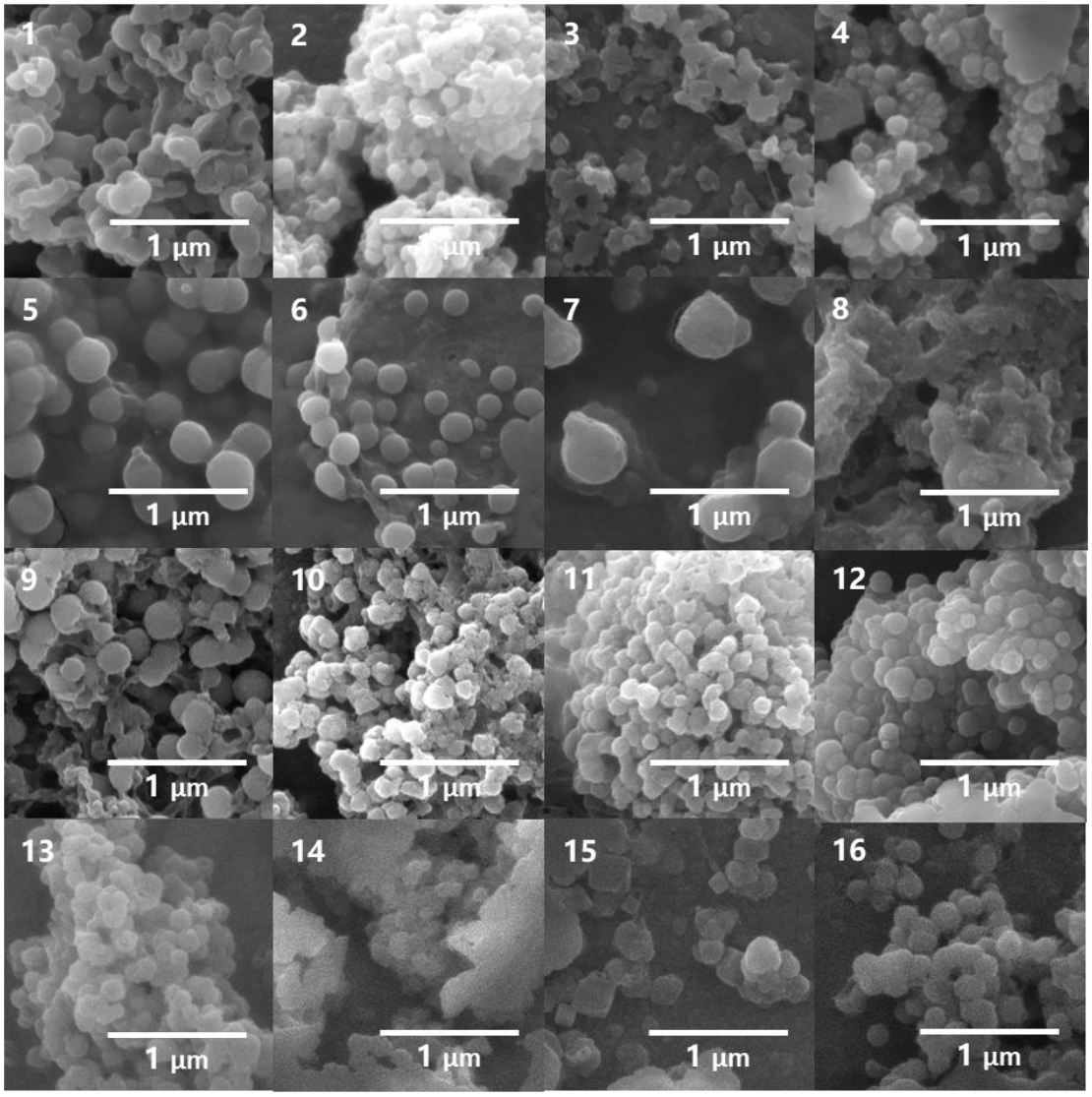

Figure 3 Morphologies of polymer synthesized in deionized water. Images 1-4 used SDS, with Lysine/IDI, Lysine/TDI, DBSA/IDI, DBSA/TDI as monomers, respectively. Images 5-8 used CTAB, with Lysine/IDI, Lysine/TDI, DBSA/IDI, DBSA/TDI as monomers, respectively. Images 9-12 used DDSA, with Lysine/IDI, Lysine/TDI, DBSA/IDI, DBSA/TDI as monomers, respectively. Images 13-16 used DOWFAX, with Lysine/IDI, Lysine/TDI, DBSA/IDI, DBSA/TDI as monomers, respectively.

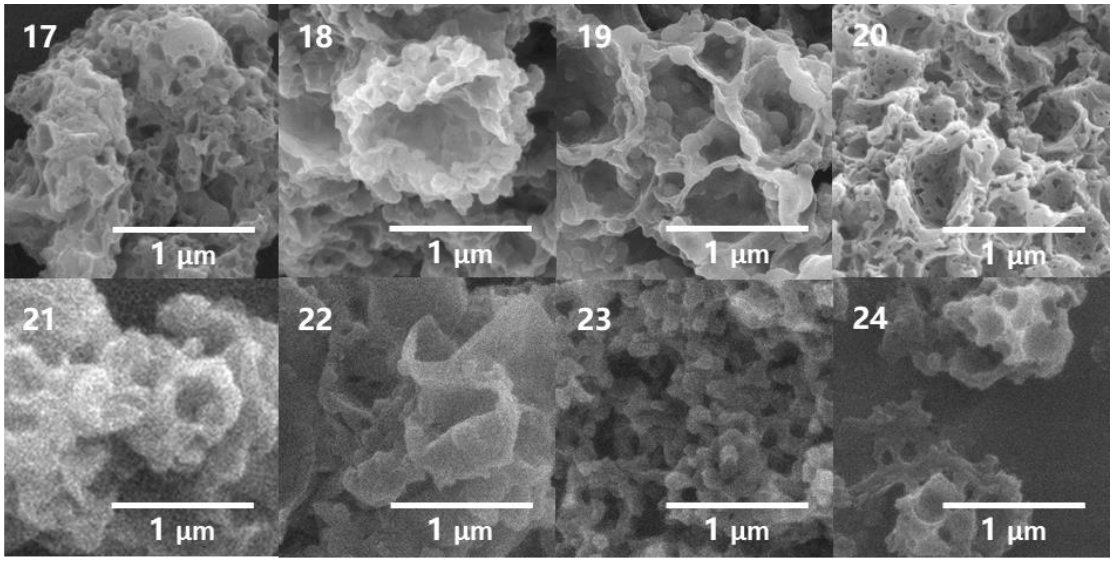

Figure 4 Morphologies of polymer synthesized in saline water. 17-20 used DDSA, with Lysine/IDI, Lysine/TDI, DBSA/IDI, DBSA/TDI as monomers, respectively. Images 21-24 used DOWFAX, with Lysine/IDI, Lysine/TDI, DBSA/IDI, DBSA/TDI as monomers, respectively.

The morphologies resulting from different synthesis mainly fall into two categories: spheres and porous structures. As shown in the SEM images, among surfactant, monomer, and aqueous phase salinity, aqueous phase salinity appears the most determining factor on nanoparticle morphology. Materials produced in deionized water, regardless of other ingredients, mostly exhibited spherical morphology, while materials produced in saline salinewater are more aggregated and porous structures. This difference might be caused by the instability of the micelles and droplets in saline water, which resulted in coalescence and breakage of the polymer membrane. Unless otherwise stated, all the following synthesis experiments were conducted in deionized water.

2.2.2. Influence of Surfactant Type

The criteria used for surfactant selection is emulsion stability. The nanocapsules need to stay well dispersed in order to maintain small enough size to pass through the pores of the formation before acid release. Stability experiments under three different conditions was evaluated: Deionized water/room temperature (DI/RT), saline water/room temperature (SW/RT), and saline water/high temperature (SW/HT). DI/RT represents the conditions for nanocapsule storage, SW/RT simulates the conditions where the nanocapsules are mixed with underground salinewater before being injected into the reservoir, and SW/HT represents the conditions into the reservoir. Only samples tested under DI/RT conditions were stable across the board. Most other samples either had observable precipitation or phase separated. The one exception was the sample prepared with CTAB and Lysine/IDI which was stable at high temperature in salinee water for a considerable amount of time.

Table 3 Result for stability test.

Surfactant	Monomer1	Monomer2	DI/RT	SW/RT	SW/HT
SDS	Lysine	IDI	Stable	Not Stable	Not Stable
SDS	Lysine	TDI	Stable	Not Stable	Not Stable
SDS	DBSA	TDI	Stable	Not Stable	Not Stable
CTAB	Lysine	IDI	Stable	Stable	Stable
DDSA	Lysine	IDI	Stable	Stable	Not Stable
DOWFAX	Lysine	TDI	Stable	Not Stable	Not Stable
DOWFAX	DBSA	TDI	Stable	Not Stable	Not Stable

2.2.3. Influence of Monomer Type and Concentration

According to the preliminary stability tests, the lysine/IDI monomer combination yielded the best results. Our next step was to optimize the monomer content in the aqueous phase in order to achieve best stability, nanostructure, and size. Sixteen combinations of aspartic acid, lysine, and DETA were tested. These three particular monomers were chosen because each of them has 1, 2, 3 amino groups, and 2, 1, 0 carboxyl groups, respectively, which may result in different crosslinking densities and colloidal stability. The results of the stability tests are shown in Figure 5 and Figure 6. Out of all the samples tested, the most stable one contains 100% lysine, which didn't phase-separate under SW/RT conditions for more than 20 hours, and remained stable under SW/HT conditions for 60 minutes. It also has the highest capsule yield according to Figure 7. The sizes of the nanostructures from different protocols are depicted in Figure 8. A large size implies aggregation of polymer, which leads to poor stability. A small size means that there is little space inside the capsules or the formation of solid spheres, which leads to low encapsulation of the acid precursor. In conclusion, the optimized monomer content in the aqueous phase is the one containing 100% lysine.

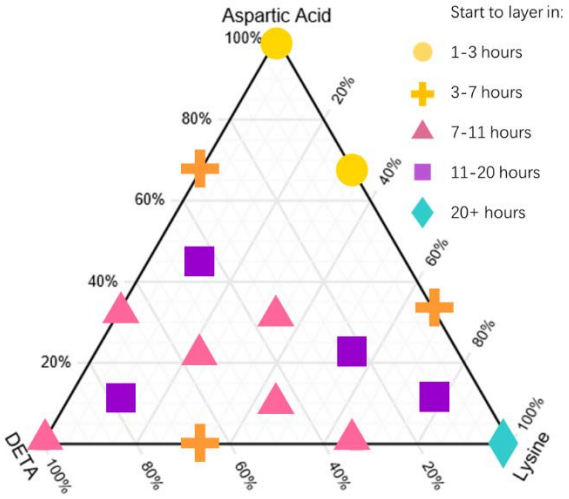

Figure 5 Emulsion stability test in saline water at room temperature.

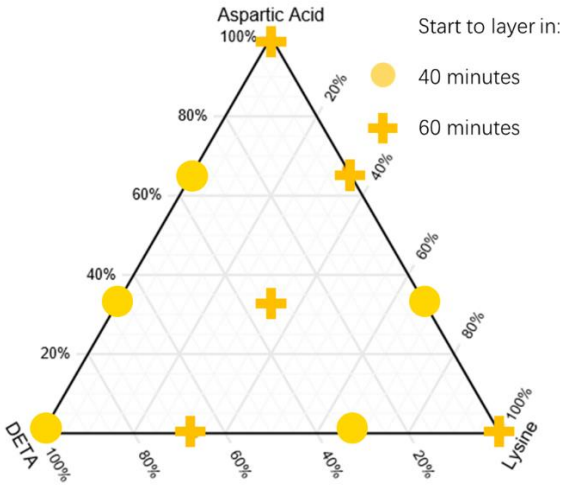

Figure 6 Emulsion stability test in saline water at 80° C.

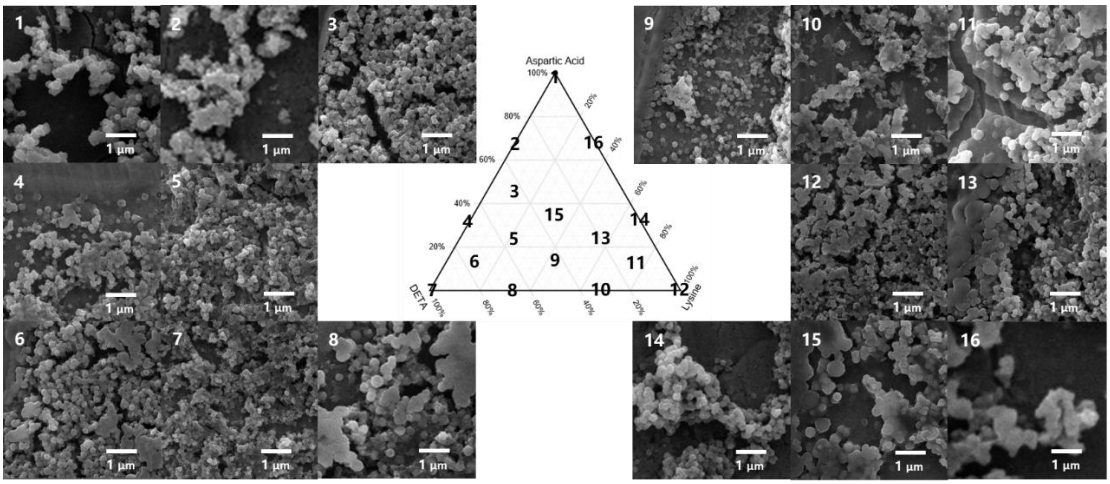

Figure 7 SEM images and the corresponding yield of nanocapsules.

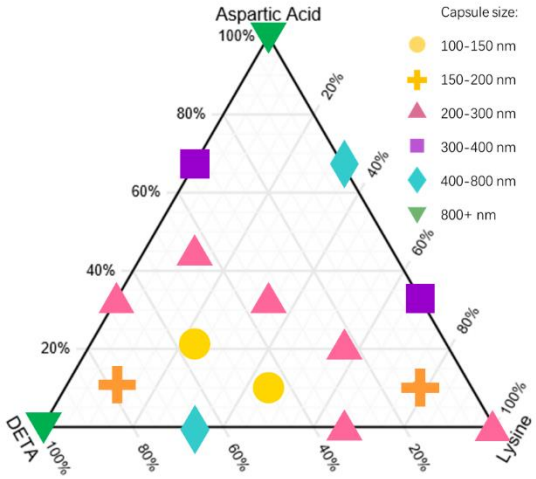

Figure 8 Size of nanocapsules synthesized different amounts of monomer

The effect of initial monomer concentration on particle size was studied by increasing the initial monomer concentration from 0.08mol/l to 0.6mol/l of lysine. Figure 9 shows that the smallest nanocapsule size is around 200 nm, and is achieved using 0.18mol/l of lysine.

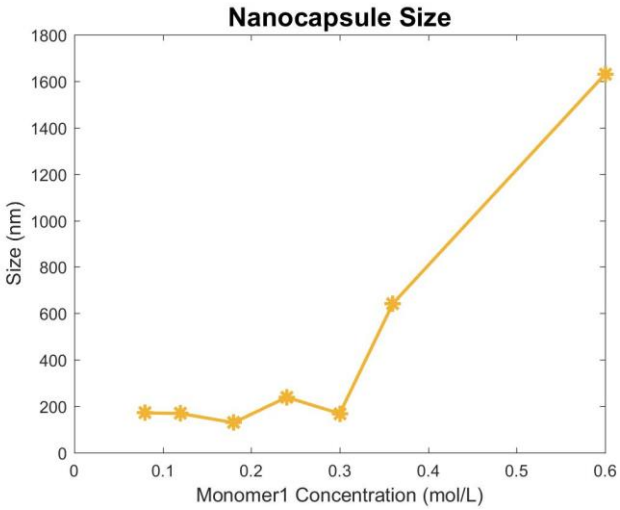

Figure 9 Nanocapsule size versus monomer 1 concentration. The molar ratio between monomer 1 and monomer 2 was fixed (specify the ratio) .

2.2.4. Acid Precursor Selection

Acid precursor selection was based on the following two requirements: a) the ability to release acid and b) emulsification capability. The desired acid precursor should remain stable during storage and transportation and react with water at high temperatures at a rate slow enough for the nanocapsules to travel deep into the oil field. After reacting with the carbonate rock, the resulting saline then can act as a surfactant to facilitate the emulsification of trapped oil.

As stated previously, surfactants with sulfonate group have been proven to exhibit satisfactory performance under harsh conditions (high salinity and high temperature). In addition, hydrochloric acid is reported to be the most commonly used in acid stimulation treatments. Taking both factors into consideration, we selected the following sulfonic chlorides candidates (listed in Table 4).

Table 4 Acid precursors used in this work.

Name	Structure
1-octanesulfonyl chloride	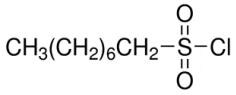
1-dodecanesulfonyl chloride	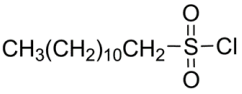
1-hexadecanesulfonyl chloride	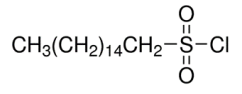

4-tert-butylbenzenesulfonyl chloride	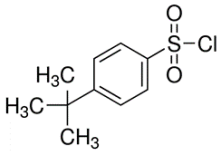
biphenyl-4-sulfonyl chloride	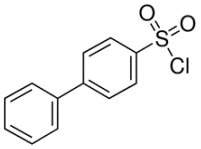

The emulsifying ability test of the hydrolyzed acid precursors was evaluated first. Crude oil was mixed with water or hydrolyzed acid precursors, and images were taken after a certain period of time. The results demonstrate that, for alkyl sulfonyl chlorides, acid precursors with longer alkyl chain length were able to keep the emulsion stable for a longer time and they also performed better than aryl sulfonyl chlorides.

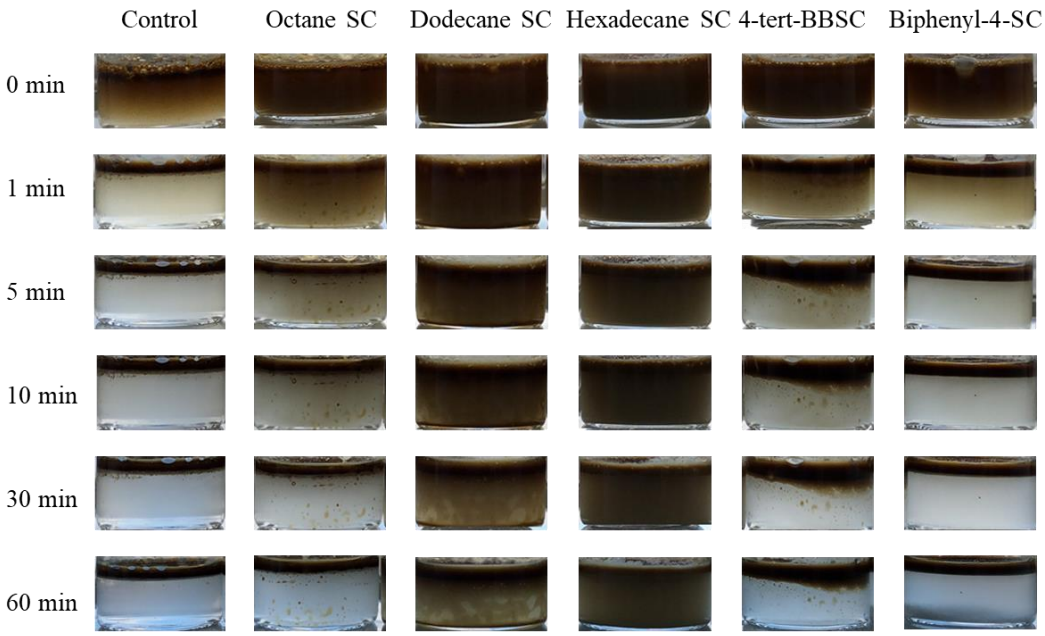

Figure 10 Emulsifying ability of fifferent acid precursors after hydrolysis.

Acid precursors with slower hydrolysis rates are considered to be more favorable for this application as they can penetrate deeper into the reservoir. The pH decrease was used to indicate the extent of hydrolysis. The result for the hydrolysis rate measurement are shown in Figure 11. After 100 minutes of reaction, the pH for most acid precursors dropped from 7 to 2, while dodecane sulfonyl chloride's was slower.

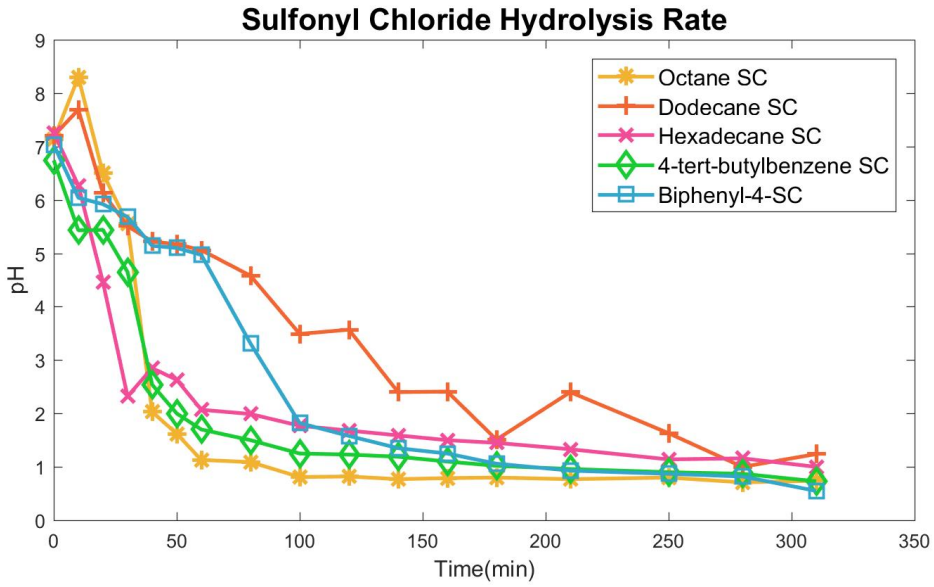

Figure 11 Sulfonyl chloride hydrolysis rate. Hydrolysis rate is corresponds to the pH drop of solution after being heated to 80° C.

In light of the above discussion, dodecane sulfonyl chloride was chosen among the candidates considering its comparatively better emulsifying ability and slower hydrolysis rate.

2.2.5. Acid Precursor Incorporated Nanocapsules

To incorporate the selected acid precursor into the nanocapsules, the acid precursor

was dissolved in the oil phase before polymerization. The scanning electron micrographs confirm that hollow spherical nanostructures were obtained after optimization.

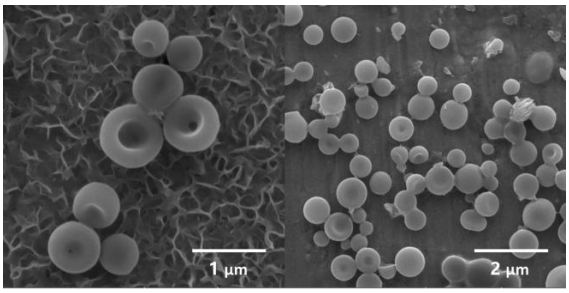

Figure 12 SEM images of nanocapsules with the acid precursor incorporated. The hollow structure of nanocapsules is shown on the left and the spherical morphology of nanocapsules on the right.

The nanocapsules were stable in either deionized water or saline water at room temperature for at least a month without any observable precipitation or phase separation. The emulsion turned clear gradually at 80°C due to the dissolution of the polymer shell.

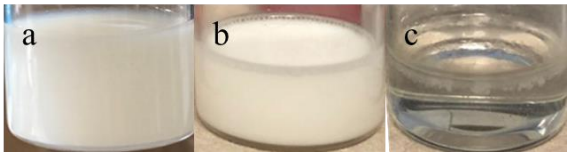

Figure 13 Nanocapsule dispersion in (a) DI/RT, (b) SW/RT, (c) SW/HT.

The hydrolysis rate test confirmed that the encapsulation slows down the acid release. As shown in Figure 15, the pH of neat precursor reached 1 afer about 150 minutes, while the encapsulated sample reached pH~2 after the same time.

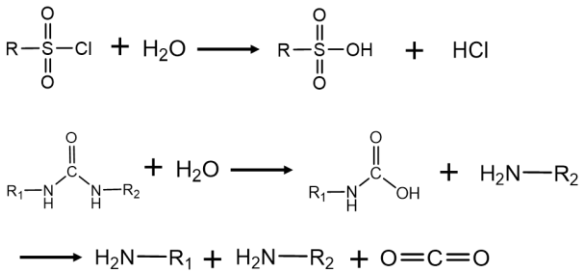

Figure 14 Schematic of hydrolysis reactions of acid precursor and polyurea shell

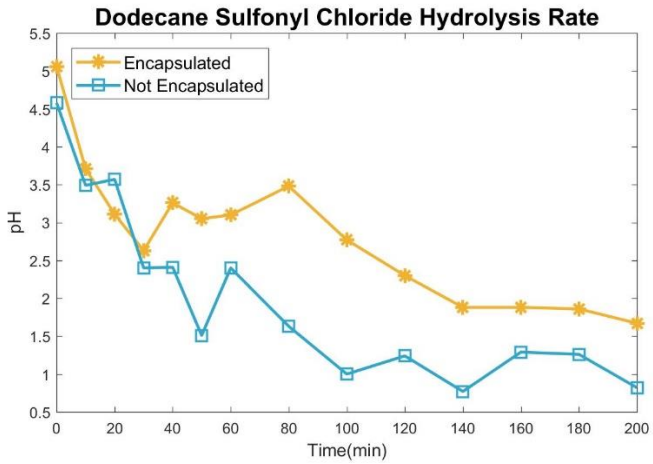

Figure 15 Dodecane sulfonyl chloride hydrolysis rate with or without encapsulation.

The emulsifying properties of hydrolyzed acid precursor encapsulated nanocapsules was tested and compared to a control sample based on an aqueous solution containing the same amount of surfactant as that derived from the fully hydrolyzed nanocapsule solution. Hydrolyzed nanocapsules enhanced the stability of crude oil in water emulsion. As shown in Figure 16, it took only 1 minute for the control sample to become almost completely phase separated, while the solution of hydrolyzed capsules reached comparable phase separation after 30 minutes or more.

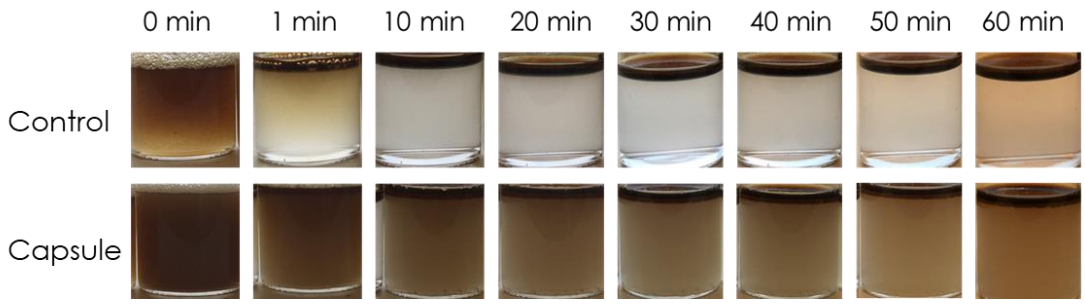

Figure 16 Emulsifying ability of hydrolyzed acid precursor incorporated into the nanocapsules.

2.2.6. Limitations

Although the acid precursor incorporated nanocapsules are proming for oil recovery application, their relatively large size remains a problem, which can only be solved at the cost of sacrificing shell thickness and volume inside the shell. Reducing shell thickness will give rise to more rapid acid release rate, and smaller volume means less acid precursor carried by each capsule. Thus, we proceeded with the second approach, in which smaller nanoparticles can be achieved to meet the requirements for EOR as described in the next chapter.

3. Solid Polymer Nanoparticles for Enhanced Oil Recovery

3.1. Materials and Methodology

3.1.1. Emulsion Polymerization

Emulsion polymerization takes place in water as the reaction medium in the presence of a non-water-soluble monomer, surfactant and initiator. Monomer emulsion is obtained by stirring and/or ultrasonication of the monomer and water mixture with the help of a surfactant.

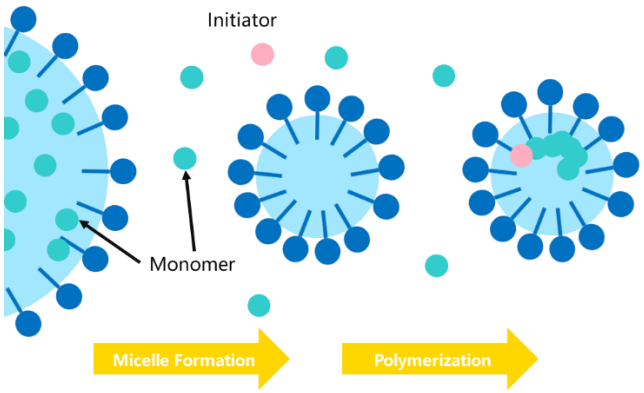

Figure 17 Schematic of Emulsion Polymerization

3.1.2. Materials Used

3.1.2.1. Surfactants

Sodium dodecyl sulfate (SDS), cetyltrimethyl ammonium bromide (CTAB), 3-(N,N-dimethylmyristylammonio)propanesulfonate (DMMAP), and 3-(N,N-dimethylstearylammonio)propanesulfonate (DMSAP) were obtained from Sigma

Aldrich. DOWFAX® 2a1 was supplied by Dow Chemical Company.

3.1.2.2. Initiators

Sodium persulfate (SPS) and Vazo 67 (V67) were obtained from Sigma Aldrich.

3.1.2.3. Comonomers

3-allyloxy-2-hydroxy-1-propanesulfonic acid sodium salt (AHPA) was obtained from Sigma Aldrich.

3.1.2.4. Oil Phase Solvent

Xylenes and butyl acetate were obtained from Sigma Aldrich.

3.1.2.5. Oil Phase Monomers

Vinyl neodecanoate (VN), vinyl laurate (VL), and vinyl acetate (VA) were obtained from Sigma Aldrich.

3.1.2.6. Saline Water

Saline water used in this section was the same as the first section.

3.1.3. Nanoparticle Synthesis

The initial synthesis protocol for solid polymer nanoparticles consisted of 15g of deionized water or saline water, 0.2g of the surfactant (or 0.4g of DOWFAX), 0.04g of the initiator, and 3g of the monomer using the following steps.

a. the ingredients for the aqueous phase, including surfactant, monomer (if

applicable), initiator (if applicable), comonomer (if applicable), and deionized water/saline water were mixed together.

b. the ingredients for the oil phase, including organic solvent (if applicable) and monomers, were mixed to form a homogeneous solution.

c. The oil phase was added into the aqueous phase while being ultrasonicated by Branson Digital Sonifier 450 and stirred for 3 minutes.

d. The mixture was stirred overnight at 400rpm and at 75°C.

3.1.4. Nanoparticle Size and Morphology

The size and size distribution of the nanoparticles as well as their morphology was characterized using the same methods as for the nanocapsules (see page **10-11** in previous chapter).

3.1.5. Stability Tests

Preliminary stability tests were conducted by letting the sample stand and observe the homogeneity of the solution over time. Diluted samples were tested by first adding 0.02g of sample solution into 10g of deionized water or saline water, then heating them up to 80°C or keeping them at room temperature and observing possible precipitation.

3.1.6. Hydrolysis Rate Measurement

The amount of polymer hydrolyzed was determined by titration. The accelerated hydrolysis tests were conducted following these steps:

a. 10g/1g of sample solution was added into 20g of deionized water and the initial pH was measured by Hanna pH meter.
b. 10g/1g of sample solution was added into excess amount of 1N/0.1N NaOH solution (20g).
c. The mixture was heated up to 85°C and stirred for a certain amount of time.
d. 1N/0.1N HCl solution was added slowly into the mixture until the pH dropped back to the initial pH, and the amount of HCl solution used was recorded.
e. From the amount of HCl consumed the percentage of polymer hydrolysed was calculated.

3.1.7. Emulsifying Ability Test

Emulsifying ability of hydrolysed nanoparticles was evaluated by the decrease in surface tension of the sample solution, which can be calculated from the contact angle between the solution and glass substrate. Contact angle measurement was carried out on Biolin Scientific Theta Lite.

3.1.8. FTIR Measurement

FTIR measurements were performed on Thermo Scientific Nicolet IS10 after the samples were dried in an oven over night and grinded.

3.2. Results and Discussion

3.2.1. Synthesis of Nanoparticles in Deionized Water

For solid polymer particle synthesis, the primary concern is the particle size and

polydispersity index (PDI). Small particle diameter ensures that the nanoparticles can pass through the porous formation in the reservoir. A narrow size dispersion curve ensures similar penetration depth for all nanoparticles in the reservoir. In this regard, we break this approach into two sections: first, synthesis of particles much smaller than 100nm in deionized water, and then functionalization of the particle surface to improve their stability in higher salinity environment.

3.2.1.1. Influence of Surfactant, Initiator and Monomer

Initially different combinations of surfactant, initiators, and monomers were tested to identify optimum reactant amounts. The resulting particle dispersion stability, particle size and PDI, were tabulated in Table 5. SDS and CTAB failed to provide stable emulsion, regardless of monomers or initiators used. On the other hand, DOWFAX is effective in stabilizing the nanoparticle dispersion. Among the combinations listed, the one based on VL, VA as monomers and sodium persulfate yielded best result, with a particle size of 72 nm and a PDI ~ 0.26.

Table 5 Reactant combinations the synthesis of solid nanoparticles

Surfactant	Monomer1	Monomer2	Initiator	Size (nm)	PDI
SDS	Dispersion not stable				
CTAB	Dispersion not stable				
DOWFAX	VN		V67	884	0.16
DOWFAX	VN	VA	V67	658	0.08
DOWFAX	VL		Sodium persulfate	108	0.11
DOWFAX	VL	VA	Sodium persulfate	72	0.26

3.2.1.2. Influence of Initiator and Surfactant Amount

The effect of initiator and surfactant was investigated by changing the amount added and measuring the size and PDI using DLS. The results are shown in Figures 18 and 19. By using larger amount of the surfactant (up to 0.6 g), particle size down to around to 65 nm was obtained. However, further increasing the surfactant amount failed to produce smaller particles, while in the meantime the PDI increased. Different amount of initiator was used in the reaction, ranging from 0.01-0.8g per sample. No significant change in size, PDI, or stability was observed within the range of 0.01-0.1g of initiator. However, with the use of 0.4g initiator, the product phase-separated after the stirring stopped, and with 0.8g initiator, the product aggregated even with stirring. Based on these results, the optimized amount of the initiator was determined to be 0.04g.

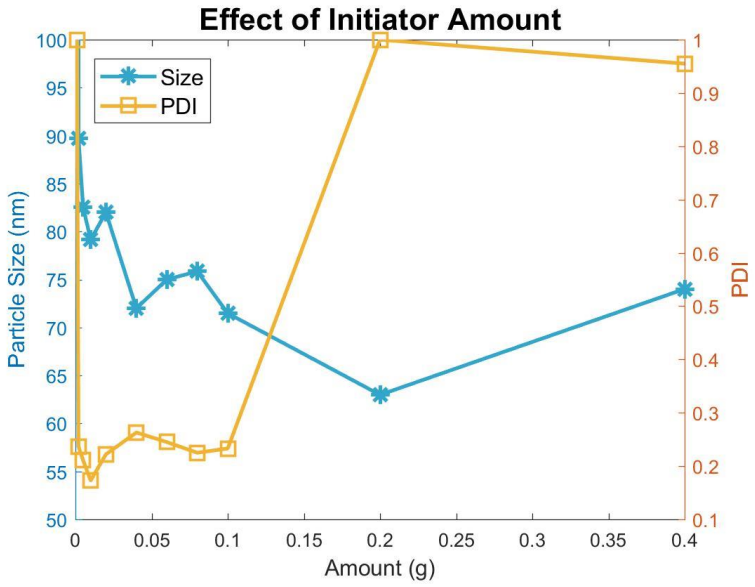

Figure 18 Effect of initiator amount on particle size and PDI.

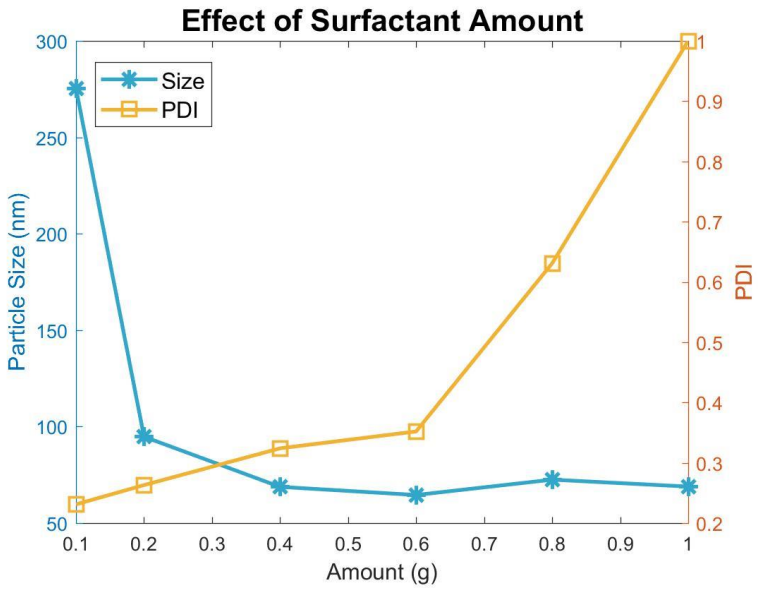

Figure 19 Effect of surfactant amount on particle size and PDI.

3.2.1.3. Influence of Monomer Ratio and Organic Solvent

We experimented with various molar ratio of VL and VA and the results are depicted in Figure 20. As the percentage of VA increases, the particle size dropped from 67nm to 48nm. However, increasing the amount of VA also caused PDI to rise from 0.35 to 0.60. Size distribution curve explains the increase of PDI with the appearance of a new peak at sizes larger than 100nm. Considering these two factors, we fixed the molar ratio between VL and VA to 3:1.

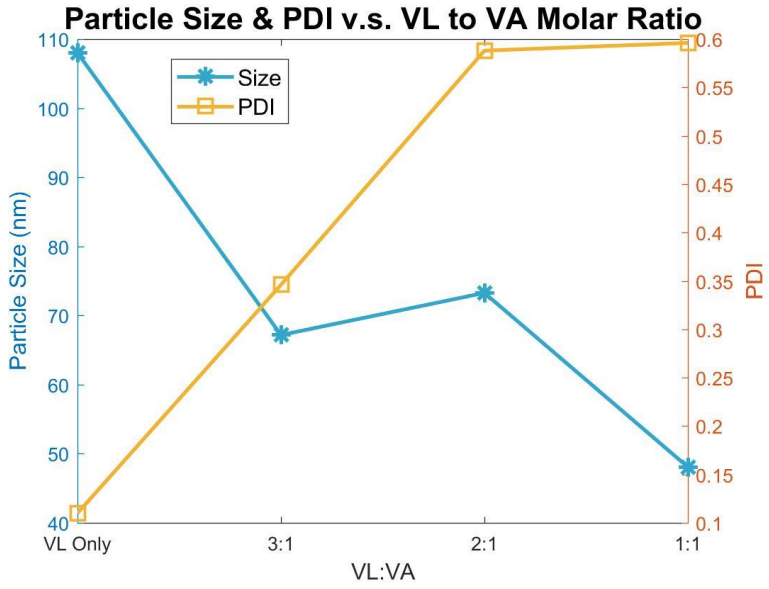

Figure 20 Particle size and PDI versus VL to VA molar ratio

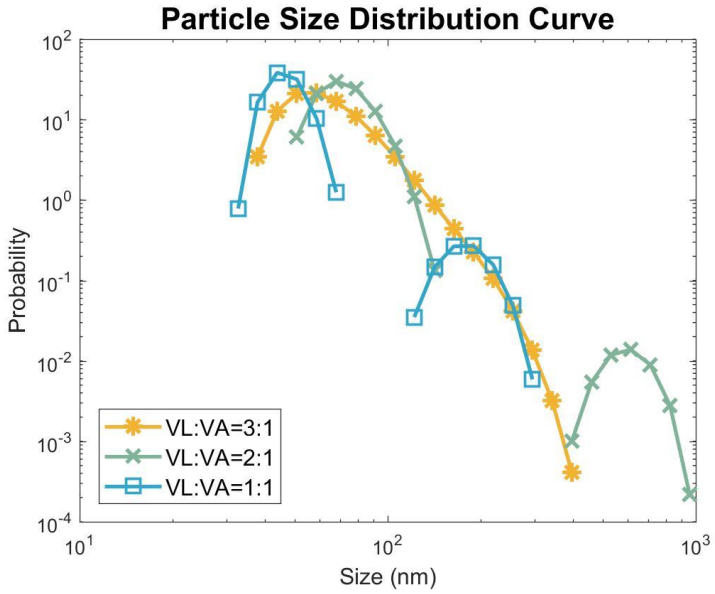

Figure 21 Particle size distribution for different VL to VA molar ratio

Following we experimented with the organic solvent. Different amount of xylene or butyl acetate was added into the oil phase before mixing with the aqueous phase while all other variables were kept the same. The results shown in Figure 22 demonstrated that xylene has the effect of decreasing both particle size and PDI,

while butyl acetate succeeded in producing more monodispersed particles, but failed in decreasing the size.

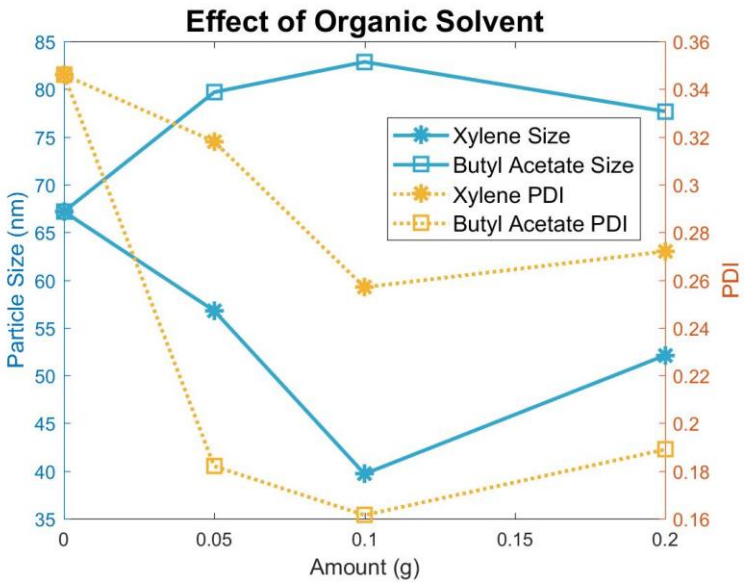

Figure 22 Effect of organic solvent on particle size and PDI.

3.2.1.4. Stability

The majority of the samples described above were able to remain well dispersed in deionized water at room temperature for at least a month. However, when these samples were added into saline water, they precipitated within 1 hour, regardless of the synthesis conditions used.

3.2.2. Synthesis of Nanoparticles in Saline Water

To keep the particles well dispersed in saline water, sulfonate groups were added to the surface by grafting sulfonated 'brushes' on the polymer spheres. Unless otherwise stated, all following experiments were conducted in saline water.

3.2.2.1. Influence of Surfactant and Comonomer

3-Allyloxy-2-hydroxy-1-propanesulfonic acid sodium salt was added into aqueous phase as the comonomer, and three types of surfactants were considered. The resulting size and stability of emulsion were tabulated in Table 6. Among three types of surfactants used, anionic surfactant DOWFAX resulted in severely phase-separated, while zwitterionic surfactants DMSAP and DMMAP were effective in keeping the particles dispersed in the emulsion. Although using DMSAP produced smaller particles, polymer aggregates were observed floating on the solution. DMMAP succeed in producing stable emulsion and the obtained latex didn't aggregate, thus DMMAP was selected for particle synthesis in saline water.

Table 6 Effect of surfactant type and comonomer amount on particle size and emulsion stability.

Surfactant	Comonomer (g)	Size (nm)	Stability
DOWFAX	0.3	101	Poor
	0.6	176	Poor
	0.9	81	Poor
DMSAP	0.3	103	Fair
	0.6	103	Fair
	0.9	106	Fair
DMMAP	0.3	138	Good
	0.6	150	Good
	0.9	157	Good

Once a feasible reaction system was established, we then focused on decreasing particle size down to 100 nm or below. We kept the components in the synthesis fixed, and changed the amount of surfactant and comonomer used. Since too much aggregates were formed in the samples using less than 0.3g of the comonomer, sizes

of those samples were not measured. It can be seen from the results shown in Table 7 that 1) that the more comonomer used the larger the particles became, and 2) the amount of surfactant added brought no significant change in particle size, yet caused a rise in PDI. The best synthesis is based on 0.16g DMMAP and 0.3g comonomer, and it produces particles with size of 138nm.

Table 7 Effect of surfactant and comonomer amount on particle size and PDI.

Surfactant \ Comonomer		0.3 g	0.6 g	0.9 g
0.16 g	**Size (nm)**	138	150	155
	PDI	0.09	0.04	0.05
0.24 g	**Size (nm)**	148	139	157
	PDI	0.13	0.07	0.05
0.32 g	**Size (nm)**	147	150	148
	PDI	0.14	0.07	0.07

3.2.2.2. Influence of Organic Solvent

Particles were synthesized following the above-mentioned recipe with or without xylene added to investigate the effect of organic solvent on particle size. Figure 23 demonstrates that in high salinity environment, xylene neither influenced the size nor the PDI of the particles produced, in contrast to the effect observed in deionized water. This might be due to the decreasing solubility of xylene in saline water, which rendered xylene ineffective in assisting monomer migration in the aqueous phase. As a result we removed xylene from the synthesis of nanoparticles in saline water.

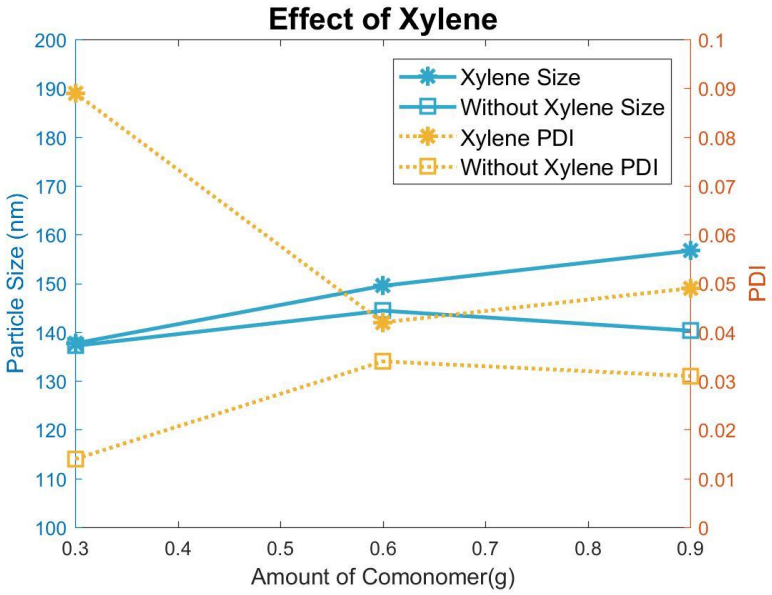

Figure 23 Effect of xylene on particle size and PDI.

3.2.2.3. Optimizing Surfactant Content

Particle size data reported in previous sections demonstrated that DOWFAX possesses the potential to help produce smaller particles. However, by itself couldn't provide stable emulsion. In an attempt to decrease particle size, we mixed different amounts of DOWFAX with 0.12g DMMAP to investigate the effect of additional DOWFAX. As illustrated in Figure 24, adding in more DOWFAX first decreased particle size, then it plateaued, with a minimum size of around 100nm. Although the addition of DOWFAX increased PDI, it's still under 0.1. Taking these considerations into account, we chose to use 0.2g of DOWFAX with 0.12g DMMAP as the optimized surfactant content.

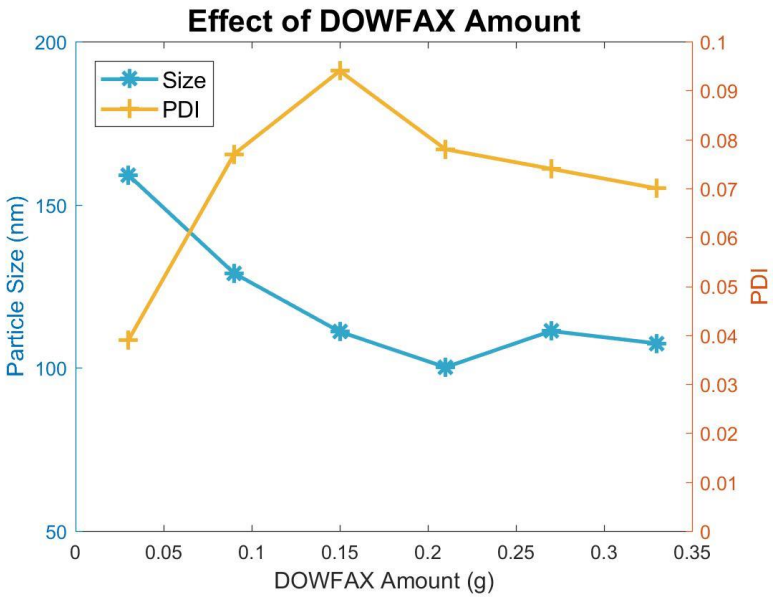

Figure 24 Effect of amount of DOWFAX on particle size and PDI.

3.2.2.4. Influence of Salinity

Particles were synthesized in different concentration of saline water following the same optimized procedure. The stability of the resulting emulsion was tested by adding those samples into excess amount of 100% saline water and observed their performance, when heated to 80°C. On the one hand, synthesizing particles in less concentrated saline water effectively decreased their size. On the other hand, the smaller particles precipitated shortly after being heated to 80°C.

We speculate that this might be due to particles synthesized in higher salinity environment had longer surface ‘brushes’, which is more favorable in stabilizing the particles in saline water. In saline water, the ‘brushes’ are more spread out compared to the ‘brushes’ in deionized water due to the interactions between cations

and sulfonate groups on the 'brushes'. If that is the case, we should observe a size difference between the same sample measured in saline water and deionized water, moreover, the size difference should increase as the salinity of the reaction medium increases. Particle size, as an indication of hydrodynamic radius, was measured in both deionized water and saline water to test this hypothesis and the difference between the particle size in the two media was measured. Figure 26 shows that the size difference did exhibit a similar trend predicted by our hypothesis.

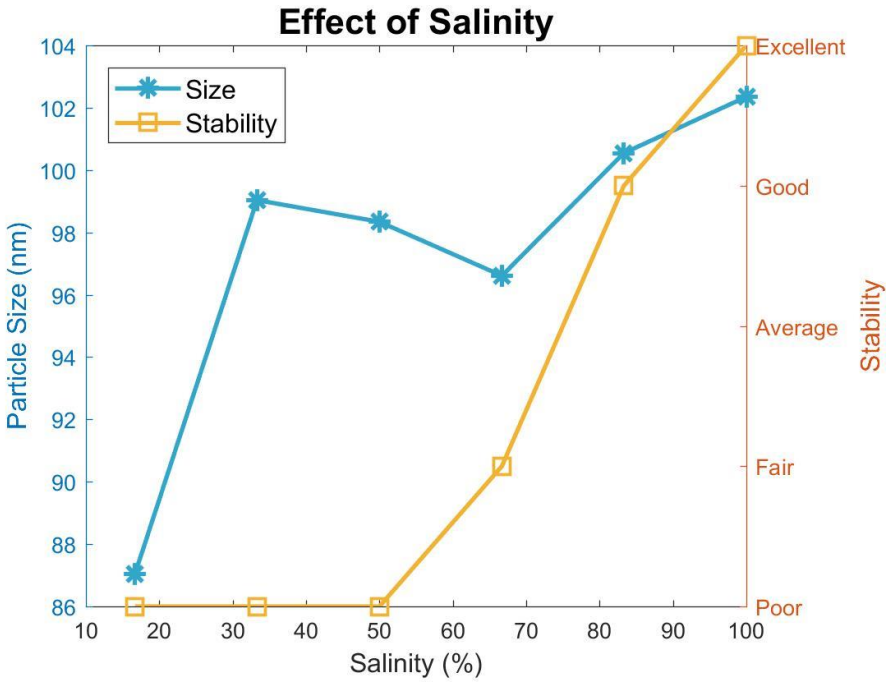

Figure 25 Effect of aqueous phase salinity on particle size and stability in saline water.

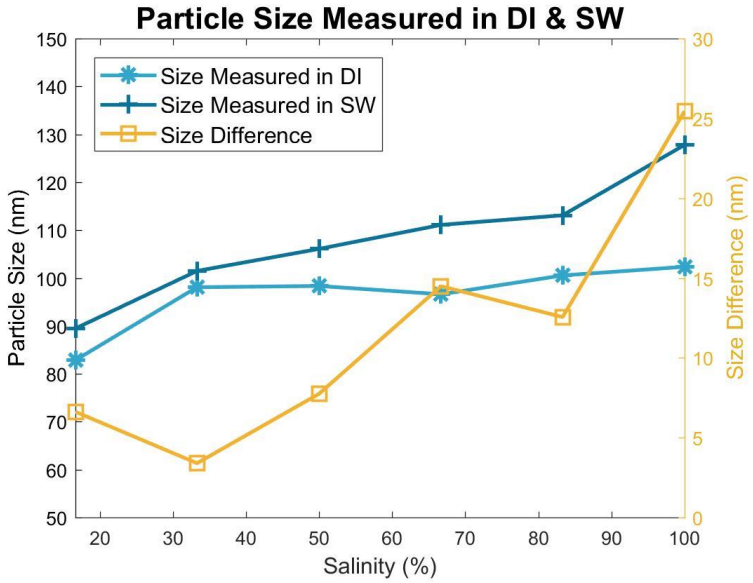

Figure 26 Particle size of samples produced in different salinity measured in both saline water and deionized water.

3.2.3. Size and Stability

The finalized procedure for solid polymer nanoparticles is listed in Table 8. Particle size measured by DLS is about 100nm. The SEM images confirm that the majority of the particles are below 100nm (Figure 27). The particles were able to stay well dispersed in saline water at 80°C for at least 30 days with no observable precipitation. The stability was further confirmed by size measurement, which showed that the particle size only increase slightly from ~102 to 130 nm over the course of this experiment.

Table 8 Recipe for solid polymer nanoparticles

Aqueous Phase					**Oil Phase**	
Surfactant		**Initiator**	**Comonomer**	**Solvent**	**Monomer**	
DOWFAX (g)	DMMAP (g)	SPS (g)	3A2h1passs (g)	Saline Water (g)	VL (g)	VA (g)
0.2	0.12	0.04	0.3	15	2.66	0.34

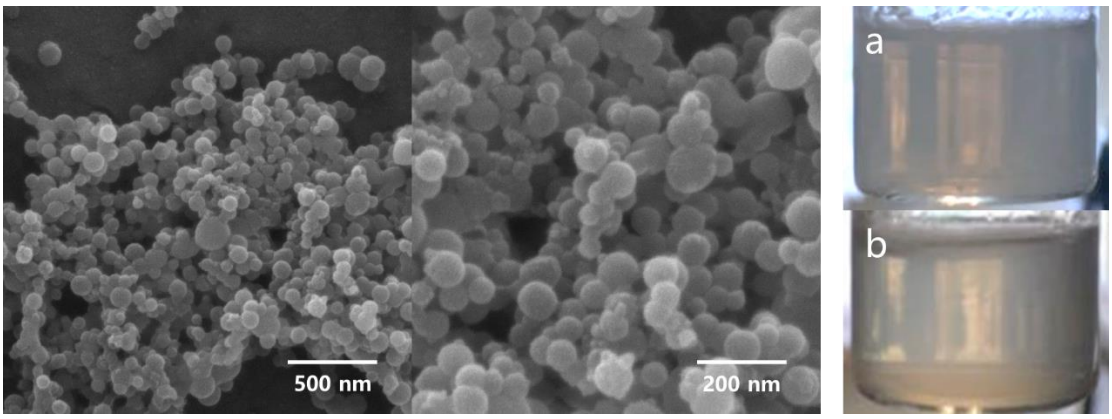

Figure 27 (Left) SEM images of nanoparticles at different magnifications. (Right) stability test in SW/HT. (a) nanoparticle dispersion after 1 hour (b) nanoparticle dispersion after 30 days.

3.2.4. Hydrolysis Tests

Accelerated hydrolysis rate measurements were conducted by using 0.1 and 1N NaOH solutions. The percentage of polymer hydrolysed was calculated using the following equation:

$$Percentage\ Hydrolyzed = \frac{Amount\ of\ NaOH\ added - Amount\ of\ HCl\ used}{Ester\ group\ in\ particles} \times 100\%$$

For the 1N NaOH accelerated reaction, 75% of total hydrolysable bonds reacted after 30 days, while for the 0.1N NaOH, only 20% reacted. These results indicated the potential of solid polymer particles of providing long time acid release at neutral pH.

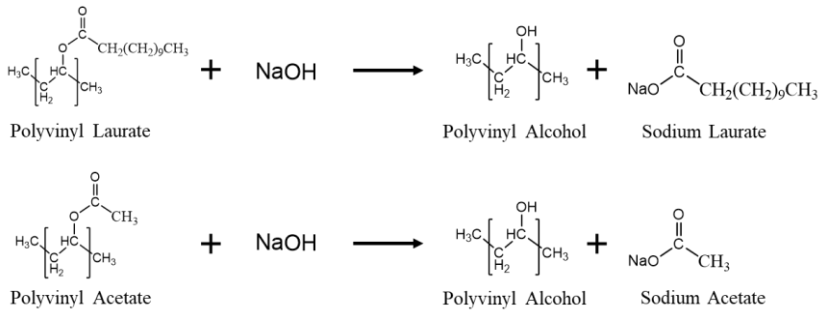

Figure 28 Schematics of hydrolysis reactions

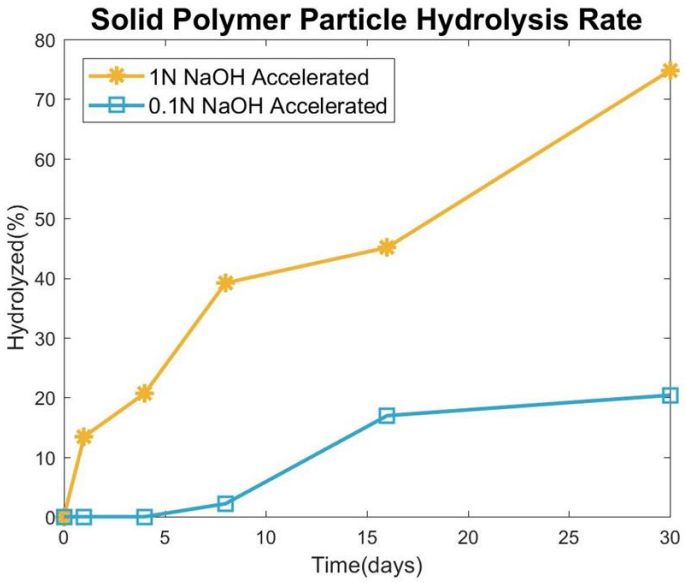

Figure 29 Solid polymer particle hydrolysis rate in 0.1N and 1 N NaOH solutions

Contact angles of the resulting solution from 1N NaOH accelerated hydrolysis reaction on cover glass were measured after 3 days and 30 days of hydrolysis and the results are presented in Figure 30. Given the surface tension of water and contact angles of different solutions with the substrate, we can calculate the surface tension of the solution after hydrolysing for a certain amount of time. [22]

$$cos\theta = -1 + 2\sqrt{\frac{\Upsilon_{sv}}{\Upsilon_{lv}}}e^{-\beta(\Upsilon_{lv}-\Upsilon_{sv})^2}$$

Where γ_{lv} is the surface tension of the solution, γ_{sv} is the surface free energy of the substrate, θ is the contact angle, and β is a constant $(0.0001247\ (m^2/mJ)^2)$

Using the contact angle of deionized water and its surface tension, we obtained the surface free energy of the piece of cover glass, with which we then plotted the relation between surface tension of the solution and cosine of contact angle. The plot shown as Figure 31 was then utilized to determine surface tension of the

solution with a given contact angle. The hydrolyzed nanoparticles had the ability of lowering surface tension by gradually increasing the surfactant concentration of the solution during the course of hydrolysis reaction. FTIR spectroscopy confirmed the disappearance of ester group and the appearance of alcohol during this process.

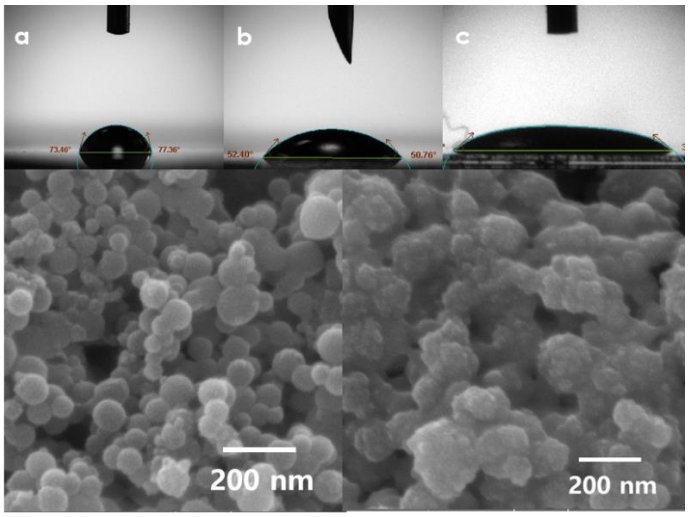

Figure 30 (Top) Contact angle between liquid and cover glass. (a) Deionized water. Contact angle was measured to be 75°, and the surface tension is 73mJ/m^2. (b) Nanoparticles hydrolyzed for 3 days. The contact angle is 52° and surface tension 54mJ/m^2. (c) Nanoparticles hydrolyzed for 30 days. Contact angle was 37° and the surface tension 46mJ/m^2. (Bottom) SEM images before and after 30 days of hydrolysis.

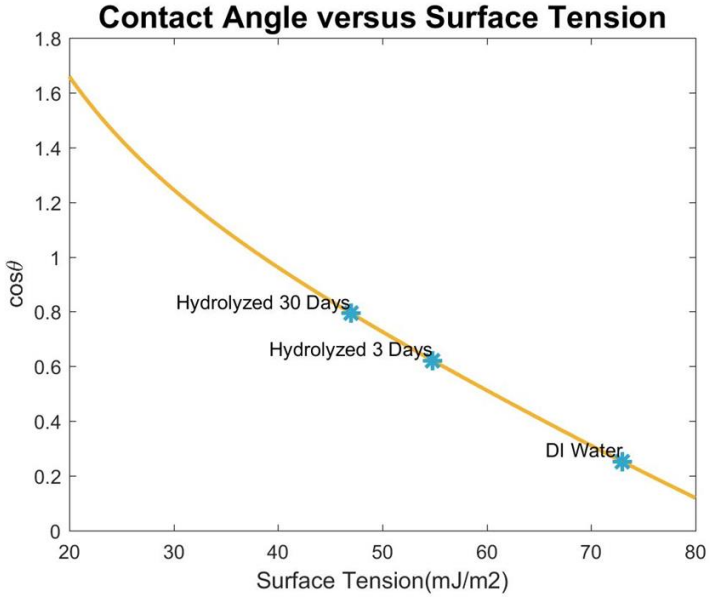

Figure 31 Relation between surface tension and cosine of contact angle.

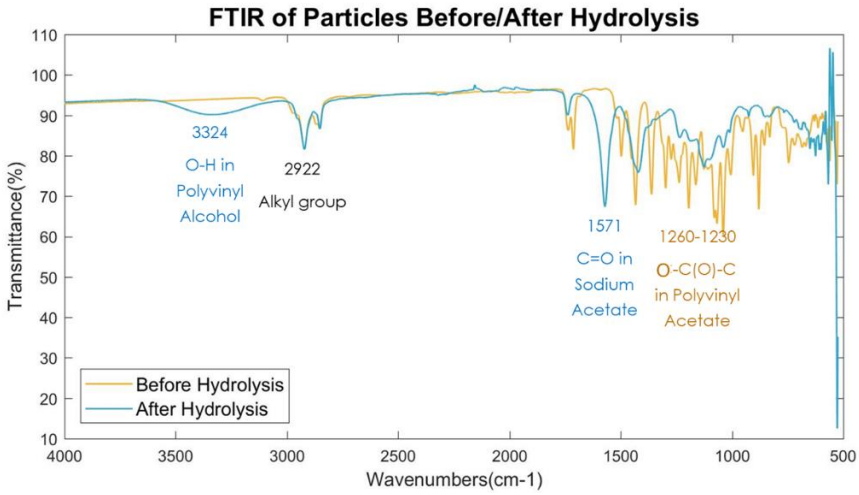

Figure 32 FTIR spectra of particles before and after 30 days of hydrolysis. The two spectra were scaled with respect to alkyl group (2922 cm^{-1}).

4. Conclusions and Recommendations

In this work, we presented two new material systems for controlled acid production and in-situ surfactant formation. The first system, acid precursor encapsulation, is based on nanocapsules with the size of 200nm, which exhibit reasonable stability in saline water at high temperature and can provide a slower release acid and meanwhile promote emulsification of trapped oil. The second system, is small solid nanoparticles of hydrolysable acid polymer of ~ 100nm. These particles are highly stable in saline water at high temperature for a considerable period of time. This new system can achieve a long- time acid release and surfactant generation under the harsh reservoir conditions.

REFRENCES

[1] "Statistical Review of World Energy (2019)"

[2] "International Energy Outlook (2017)" (PDF). EIA. 2017-09-14. p. 10.

[3] Bera, A. , & Mandal, A. . (2015). Microemulsions: a novel approach to enhanced oil recovery: a review. Journal of Petroleum Exploration and Production Technology, 5(3), 255-268.

[4] Thomas, & S. (2008). Enhanced oil recovery - an overview. Oil & Gas Science and Technology - Revue de l\"IFP, 63(1), 9-19.

[5] Kalfayan, L.J. . (2008). Production Enhancement with Acid Stimulation (Second Edition).

[6] Buijse, Marten & de Boer, Peter & Breukel, Bert & Klos, Monique & Burgos, Gerardo. (2003). Organic Acids in Carbonate Acidizing. 10.2523/82211-MS.

[7] Harris, R. E. , & Mckay, I. D. . (1998). [society of petroleum engineers european petroleum conference -, (1998.10.20-1998.10.22)] proceedings of european petroleum conference - new applications for enzymes in oil and gas production.

[8] Fredd, C. N. , & Fogler, H. S. . (1998). Alternative stimulation fluids and their impact on carbonate acidizing. SPE Journal, 3(01), 34-41.

[9] Tupã, Pedro & Aum, Pedro & Nóbrega, Talles & Souza & Aum, Yanne & Gurgel, Pereira & Gurgel Aum, Yanne & Castro, Tereza & , Dantas & Avelino, Afonso & Dantas Neto, Afonso. (2016). New Acid O/W Microemulsion Systems for Application in Carbonate Acidizing. International Journal of Advanced Scientific

and Technical Research. 6.

[10] Portier, S. & Andre, L. & D.Vuataz, F. . (2007) Review on chemical stimulation techniques in oil industry and applications to geothermal systems

[11] Kamal, M. S. , Hussein, I. A. , & Sultan, A. S. . (2017). Review on surfactant flooding: phase behavior, retention, IFT and field applications. Energy & Fuels, acs.energyfuels.7b00353.

[12] Negin, C. , Ali, S. , & Xie, Q. . (2016). Most common surfactants employed in chemical enhanced oil recovery. Petroleum, S2405656116300621.

[13] Hirasaki, G. J. . (2008). Recent advances in surfactant EOR. SPE Journal, 16(4), 889-907.

[14] Suryo, P. , & Murachman, B. . (2001). Development of Non Petroleum Base Chemicals for Improving Oil Recovery in Indonesia. Spe Asia Pacific Oil & Gas Conference & Exhibition. Society of Petroleum Engineers.

[15] Chai, J. L. , Zhao, J. R. , Gao, Y. H. , Yang, X. D. , & Wu, C. J. . (2007). Studies on the phase behavior of the microemulsions formed by sodium dodecyl sulfonate, sodium dodecyl sulfate and sodium dodecyl benzene sulfonate with a novel fishlike phase diagram. Colloids and Surfaces A: Physicochemical and Engineering Aspects, 302(1-3), 31-35.

[16] Iglauer, S. , Wu, Y. , Shuler, P. , Tang, Y. , & Iii, W. A. G. . (2010). New surfactant classes for enhanced oil recovery and their tertiary oil recovery potential. Journal of Petroleum Science & Engineering, 71(1-2), 23-29.

[17] Qiao, W. , Li, J. , Zhu, Y. , & Cai, H. . (2012). Interfacial tension behavior of

double long-chain 1,3,5-triazine surfactants for enhanced oil recovery. Fuel, 96(none), 220-225.

[18] Bai, Y. , Xiong, C. , Shang, X. , & Xin, Y. . (2014). Experimental study on ethanolamine/surfactant flooding for enhanced oil recovery. Energy & Fuels, 28(3), 1829-1837.

[19] Yow, H. N. , & Routh, A. F. . (2006). Formation of liquid core-polymer shell microcapsules. Soft Matter, 2(11), 940.

[20] Bouchemal, K. , Brian, S. , Perrier, E. , Fessi, H. , Bonnet, I. , & Zydowicz, N. . (2004). Synthesis and characterization of polyurethane and poly(ether urethane) nanocapsules using a new technique of interfacial polycondensation combined to spontaneous emulsification. International Journal of Pharmaceutics (Kidlington), 269(1), 89-100.

[21] Liang, C. , Lingling, X. , Hongbo, S. , & Zhibin, Z. . (2009). Microencapsulation of butyl stearate as a phase change material by interfacial polycondensation in a polyurea system. Energy Conversion and Management, 50(3), 723-729.

[22] Kwok, D. Y. , Lam, C. N. C. , Li, A. , Zhu, K. , Wu, R. , & Neumann, A. W. . (2010). Low-rate dynamic contact angles on polystyrene and the determination of solid surface tensions. Journal of Colloid & Interface Science, 38(10), 1675-1684.

[23] Kamal, M. S., Shakil Hussain, S. M. and Fogang, L. T. (2018), A Zwitterionic Surfactant Bearing Unsaturated Tail for Enhanced Oil Recovery in High-Temperature High-Salinity Reservoirs. J Surfactants Deterg, 21: 165-174.

doi:10.1002/jsde.12024